



Research papers

Complementary Relationship for evaporation performance at different spatial and temporal scales

Richard D. Crago^{a,*}, Russell Qualls^b, Jozsef Szilagyi^{c,d}^a Bucknell University, Lewisburg, PA, USA^b University of Idaho, Moscow, ID, USA^c Budapest University of Technology and Economics, Budapest, Hungary^d University of Nebraska-Lincoln, Lincoln, NE, USA

ARTICLE INFO

This manuscript was handled by Marco Borga, Editor-in-Chief, with the assistance of Lixin Wang, Associate Editor

Keywords:

Evaporation

Scaling

Potential evaporation

Complementary relationship

ABSTRACT

Several versions of the Complementary Relationship (CR) between actual regional evaporation and apparent potential evaporation have recently been proposed. Few studies have compared multiple CR versions side-by-side using datasets spanning various climates and land surfaces. Filling this lack is one purpose of this project. It also investigates how various CR versions respond to changes in spatial and temporal averaging. This study uses multiple years of data from seven eddy-covariance flux stations in Australia, representing a wide range of biomes, along with global ERA5 reanalysis data products. Daily and monthly averages were used for both datasets, and the Australian observations also used weekly and yearly averages. The ERA5 data represent a scale of about 30 km, much larger than the scale represented by the flux station data. A set of five questions regarding the impact of spatial and temporal scaling on CR parameter values and performance are asked and assessed using the two datasets. Four recent CR versions are considered in answering the questions. Due to important differences between FLUXNET and ERA5 data, questions regarding temporal scaling were answered with greater confidence than those regarding spatial scaling. With these data, rescaled versions of the CR performed best overall.

1. Introduction

The Complementary Relationship (CR) (Bouchet, 1963) between actual regional evaporation (or latent heat flux, LE) and apparent potential evaporation—evaporation under actual radiation, temperature, humidity and wind conditions but with a saturated surface (LE_p)—has taken many forms over the years (Brutsaert, 1982, 2005). In all of them the main idea is that the humidity of the atmospheric boundary layer (ABL) over a region will reflect the rate of humidity entering the ABL through surface evaporation, such that surfaces with a high evaporation rate tend to have high humidity, and those with low evaporation rates tend to have low humidity. Recently, Brutsaert (2015) introduced the concept of a generalized complementary relationship based on physical analysis of the saturated and desiccated regional surface boundary conditions. Since then, new versions of the CR adapted from Brutsaert's (2015) work have appeared in the literature, including those by Han and Tian (2018, 2020), Crago et al. (2016), and Szilagyi et al. (2016, 2017).

While each of these CR versions has undergone a validation process, a more comprehensive side-by-side comparison of these versions under a

range of climate and land surface conditions is needed. The primary goal of this study, however, is to investigate how changes in temporal averaging periods and spatial averaging scales affects each of the CR versions. It is clear that spatial and temporal scaling play an important role in the physical processes behind the CR, so that slightly different formulations are appropriate for different spatial and temporal scales. For example, Crago et al. (2016) and Szilagyi et al. (2016) both used versions of the “rescaled” CR proposed by Crago et al. (2016), but fit the data with different functional forms. Szilagyi et al. (2017) and Han and Tian (2020) have speculated that these scaling issues could be important. If so, then different data sets might have different behavior depending on their spatial and temporal scales, resulting in different CR versions for the different scales. An understanding of how CR models behave at various spatial and temporal scales is essential for the reliable and routine application of global estimates of evaporation using a CR model. The feasibility of global estimates using CR models has been clearly established, as has the ability of these models to illuminate global spatial and temporal evaporation trends (Brutsaert et al., 2020; Ma et al., 2021).

* Corresponding author.

E-mail address: rcrago@bucknell.edu (R.D. Crago).

A key assumption behind the CR is that the atmosphere is well-adjusted to the evaporation rate of the underlying surface, but many of the forcing variables change considerably over the diurnal cycle. Furthermore, atmospheric stability and the evolution of the atmospheric boundary layer (ABL) also have a pronounced diurnal cycle (e.g., Stull, 1988; Brutsaert, 2005). It might be reasonable to assume that the ABL is well-adjusted to the underlying surface for a day as a whole (e.g., Brutsaert, 2015). But many of the equations that make up the CR are non-linear, so it is not entirely clear what role different averaging periods might have.

With respect to spatial averaging, Monin-Obukhov similarity theory requires a homogeneous surface upwind of a measurement for a sufficient fetch (e.g. Stull, 1988). Thus, flux measurement sites should ideally be carefully chosen to have sufficient fetch in the direction of the prevailing wind, so that the measured fluxes represent a fairly clearly-defined surface area. However, in hilly terrain or regions with complex patterns of vegetation cover, it is not always clear how to choose a measurement site representative of the varied regional surface. Since many natural and managed landscapes have these complex patterns, point measurements of latent heat fluxes, typically representative of footprints over length scales of order 10^2 to 10^3 m, may not be representative over a larger region, such as a watershed or a cell in a numerical atmospheric model.

This study is a preliminary assessment of five questions regarding the CR applied at different spatial and temporal scales:

1. As either the spatial or temporal scale increases, will the averaging process reduce the effect of extreme values so that CR model errors decrease?
2. As the temporal scale increases, will the range of data values be compressed by the averaging process so that CR model estimates of evaporation also have a compressed range?
3. As spatial scales increase, will the impact of small-scale advection due to inhomogeneous surfaces decrease?
4. Do the CR versions that provide the best estimates of dimensionless evaporation (evaporation divided by apparent potential evaporation) also provide the best predictions of dimensional (actual) evaporation?
5. Are there CR versions that perform particularly well, and if so, are there characteristics that these specific CR versions have in common?

In order to address these questions, data derived from four temporal averaging periods (daily, weekly, monthly, and yearly) and two different spatial scales will be used to estimate actual evaporation using four different CR formulations (versions). The different spatial scales will be obtained by using eddy covariance fluxes from surface stations along-side global reanalysis data, and temporal scales will be obtained through different averaging periods. Trends of parameter values [e.g., the Priestley & Taylor (1972) parameter α] and model performance statistics with different averaging periods and areas will be analyzed to address the five questions.

2. Materials and methods

An overview of the CR, the underlying equations, and several recent CR formulations will be presented first, and then the data sources will be discussed.

2.1. Equations

The land surface energy budget can be written (Brutsaert, 1982, 2005):

$$R_n - G = H + LE \tag{1}$$

where R_n is the net radiation input, G is the heat flux into the ground, H

is the sensible heat flux into the atmosphere, and LE is the latent heat flux into the atmosphere (which will often be denoted as evaporation).

Penman (1948) derived an approximate equation for wet surface evaporation:

$$LE_{pen} = \frac{\Delta}{\Delta + \gamma} (R_n - G) + l_v \frac{\gamma}{\Delta + \gamma} E_A, \tag{2}$$

where $\Delta = de^*(T)/dT$ evaluated at the air temperature (T_a) at height z_T , γ is the psychrometric constant, l_v is the latent heat of evaporation, and E_A is the drying power of the air, given by:

$$E_A = f(u)[e^*(T_a) - e_a], \tag{3}$$

where u is the wind speed, e_a is the vapor pressure at height z_T , and $e^*(T_a)$ is the saturation vapor pressure at air temperature. Vapor pressure is given by (e.g. Chow et al., 1988):

$$e^*(T) = c_1 \exp\left(\frac{c_2 T}{c_3 + T}\right), \tag{4}$$

where e^* is in Pa, T is in $^{\circ}C$, and c_1 , c_2 , and c_3 are equal to 6.1365, 17.502, and 240.97 for $T \geq 0^{\circ}C$, respectively, and to 3.1539, 22.452 and 272.55, respectively for $T < 0^{\circ}C$ (Andreas et al., 2013). Finally, the wind function in E_A is given by Brutsaert (2005):

$$f(u) = \frac{0.622k^2 u}{R_d T_a \ln[(z_T - d)/z_{0v}] \ln[(z_u - d)/z_0]}, \tag{5}$$

where $k = 0.4$ is von Karman's constant, R_d is the ideal gas constant for dry air, d is the displacement height, z_{0v} is the scalar roughness length for water vapor, and z_0 is the momentum roughness length. Other formulations for $f(u)$ will be considered later. LE_{pen} is considered to be a good estimate of apparent potential evaporation, LE_p (e.g., Brutsaert, 2015; Brutsaert and Stricker, 1979; Han and Tian, 2018; Brutsaert, 1982; Brutsaert, 2005).

If the vapor pressure deficit [$e^*(T_a) - e_a$] over a large saturated surface goes to 0, (2) implies $LE_{pen} \rightarrow LE_e$, where

$$LE_e = \frac{\Delta}{\Delta + \gamma} (R_n - G). \tag{6}$$

This LE_e is known as equilibrium evaporation (Slatyer and McIlroy, 1961). Priestley and Taylor (1972) noted that, even for very large saturated surfaces, the air rarely reaches saturation, so they introduced $\alpha > 1$ to account for warm, dry advection:

$$LE_{PT} = \alpha LE_e. \tag{7}$$

Priestley and Taylor (1972) found an average of $\alpha = 1.26$ from a number of large wet surfaces.

Originally (Priestley and Taylor, 1972), Δ in Eq. (10) was taken to be the slope de^*/dT evaluated at the wet-environment air temperature T_{wa} . Szilagyi and Jozsa (2008) argued that T_{wa} is usually close to the wet surface temperature T_{ws} . Szilagyi and Schepers (2014) demonstrated that T_{ws} remains nearly constant in space and time for a wet surface (independent of areal extent) within a drying region if the wind speed and $R_n - G$ have little variability. This way T_{ws} can be found for a small wet patch by setting two expressions for the wet surface Bowen ratio equal to each other (e.g., Szilagyi, 2015) and solving (using a numerical equation solver) for T_{ws} :

$$B_o = \frac{R_n - G - LE_{pen}}{LE_{pen}} = \gamma \frac{T_{ws} - T_a}{e^*(T_{ws}) - e(T_a)}. \tag{8}$$

Then T_{wa} should be the lesser of T_{ws} and T_a (Szilagyi, 2015); in practice, with these data, $T_{wa} = T_{ws}$.

Thus, LE_{PT} in (11) calculated using $\Delta(T_{ws})$ (i.e. de^*/dT evaluated at T_{ws}) represents the evaporation rate of a wet surface having a regional extent allowing it to influence the air temperature over it via surface cooling. In this study, versions of equilibrium evaporation (6) will make

use of Δ calculated at T_{ws} and at T_a which will be denoted $\Delta(T_{ws})$ and $\Delta(T_a)$, respectively.

The CR versions considered herein find their root in the work of Brutsaert (2015). He developed a generalized complementary relationship, given by:

$$y_B = 2x^2 - x^3, \tag{9}$$

where $x = LE_w/LE_p$, $y = LE/LE_p$, y_B is an estimate of y , LE_w is the evaporation rate of a large saturated surface (usually taken to be LE_p —see Brutsaert and Stricker, 1979) and LE_p is the apparent potential evaporation rate given by (2). The functional form of (9) is the simplest polynomial that can satisfy the four boundary conditions proposed by Brutsaert (2015), namely $x = 0$ at $y = 0$, $x = 1$ at $y = 1$, $dy/dx = 0$ at $y = 0$, and $dy/dx = 1$ at $y = 1$. (Note that all the CR versions tested here are formulated in dimensionless form, that is, in terms of x and y .)

Crago et al. (2016) noted that $y = 0$ does not imply $x = 0$ because even for a completely dry region, LE_p cannot go to infinity [see (2)]. They suggested that $y \rightarrow 0$ at $x_{min} = LE_w/LE_{max}$, where LE_{max} is the value of LE_p expected for a desiccated regional surface. Since LE_p is found with (2), this same equation should also be used to estimate LE_{max} . Following Szilagyi et al (2016), LE_{max} is defined using (2), where $e_a = 0$, $e^*(T_a)$ is replaced by $e^*(T_{dry})$, Δ is replaced by $\Delta = d(e^*)/dT$ evaluated at T_{dry} , and $T_{dry} = T_a + e_a/\gamma$. Thus, x_{min} is found from LE_{PT} divided by this LE_{max} .

Thus, x does not range from 0 to 1 but only from x_{min} to 1. Crago et al. (2016) suggested rescaling x to X :

$$X = \frac{x - x_{min}}{1 - x_{min}}, \tag{10}$$

which does range from 0 to 1. Crago et al. (2016) suggested the CR could be represented as

$$y = X. \tag{11}$$

Since LE_{max} is different for each data point, so is x_{min} , so that data plotted on an (x, y) graph are rearranged horizontally when plotted on an (X, y) plot. Szilagyi et al. (2016) suggested the use of (9) with x replaced by X from (10), combining the boundary conditions proposed by Brutsaert (2015) with the rescaling of (10).

Han and Tian (2018) proposed a sigmoid-shaped curve in x - y space:

$$y_{HT} = \frac{1}{1 + m \left(\frac{x_{max} - x}{x - x_{min}} \right)^n}, \tag{12}$$

where

$$n = \frac{4\alpha(1 + 1/b_{HT})(x_{0.5} - x_{min})(x_{max} - x_{0.5})}{x_{max} - x_{min}} \tag{13}$$

and

$$x_{0.5} = \frac{0.5 + 1/b_{HT}}{\alpha(1 + 1/b_{HT})}, \tag{14}$$

with b_{HT} a second model parameter and

$$m = \left(\frac{x_{0.5} - x_{min}}{x_{max} - x_{0.5}} \right)^n. \tag{15}$$

In practice, Han and Tian (2018, 2020) recommend $x_{min} = 0$ and $x_{max} = 1$. Their parameter α is loosely related to the Priestley-Taylor parameter, but it primarily establishes the slope of the sigmoid curve at the center of the graph. Both α and b_{HT} must be specified or calibrated. Equation (12) is explicitly based on the two terms of Penman’s equation, so in their model x is taken as $LE_e(T_a)/LE_{pen}$ and y is LE/LE_{pen} .

The focus of this study is on the different broader versions of the CR (i.e. strategies for finding y from x). Specifically, there are four of these versions: First, Brutsaert’s (2015) equation (9) giving estimates y_B ; second the rescaled relationship (11) with (10) giving estimates X ; third, the use of the rescaled variable x (10) to replace x in (9) giving estimates

X_B ; and Han and Tian’s (2018) method based on equations (12)-(15) giving estimates y_{HT} .

Research regarding the CR is evolving rapidly; each of the CR versions presented here has been the subject of debate in the literature (e.g, see Ma and Zhang, 2017; Ma and Szilagyi, 2019; Szilagyi and Crago, 2019; Han and Tian, 2020; Liu et al., 2020, Crago et al., 2017; Crago et al., 2020a; Crago et al., 2020b; Crago et al., 2021). Thus, there is a need for studies testing multiple versions of the CR with a variety of datasets from a variety of sites around the world. This project is intended to partly fill this gap.

These four versions, and the notation used in defining them, are found in Table 1. Dimensional evaporation (LE_X , LE_B , LE_{XB} , and LE_{HT} , in $W\ m^{-2}$) is derived from dimensionless evaporation (X , y_B , X_B , and y_{HT} , respectively) by multiplying the dimensionless rate by LE_{pen} . Reference values will be described in the next section, but dimensional reference evaporation values are denoted LE_r , and dimensionless values are denoted y_r . Table 1 also indicates which temperature is used to calculate Δ in (6) for each version.

2.2. Data sources

Data from two sources were used in this study as described below.

2.2.1. FLUXNET

Data from seven FLUXNET (Baldocchi et al., 2001) sites in Australia (see Crago and Qualls, 2018 for details of the sites) were used here. These eddy-covariance flux stations measured net radiation, sensible heat flux and latent heat flux, ground heat flux, atmospheric pressure, air temperature, vapor pressure deficit, wind speed, and friction velocity. Crago and Qualls (2018) used the friction velocity values to find an optimum value of z_0 for each site; these are the values used here. The sites ranged from tropical to temporal, arid to humid, and included a large seasonal wetland, a tropical savannah, and tall temporal forests. Daily, weekly, monthly, and yearly average data products are available from FLUXNET (<http://fluxnet.fluxdata.org/>). The energy budget closure problem was resolved by forcing the measured Bowen ratio to hold, and finding reference values of H_r and LE_r that satisfy the energy budget (1). Because averaging periods up to a year were used, gap-filling techniques provided by FLUXNET (Pastorello et al., 2020) were applied.

2.2.2. ERA5

ERA5 is a reanalysis product produced by ECMWF (Hersbach et al., 2020). It is the successor to ERA-Interim (Dee et al., 2011). Reanalysis data products combine observations (e.g., radar, satellite, and station data) and model analysis to arrive at the most probable state of the atmosphere. ERA5 data are on a 30-km grid covering the globe. A land/sea mask is available to select only land surfaces (in this study, land surfaces

Table 1
Evaporation variables.

Dimensionless Variable	Dimensionless Formula	Dimensional Variable	Dimensional Formula
X	$x = \alpha LE_e(T_{ws})/LE_{pen}$ LE_r/LE_{pen} $x_{min} = \alpha LE_e(T_{ws})/LE_{max}$ $X = (x - x_{min})/(1 - x_{min})$	LE_X	$X \cdot LE_{pen}$
y_B	$x = \alpha LE_e(T_a)/LE_{pen}$, $y_r = LE_r/LE_{pen}$	LE_B	$y_B \cdot LE_{pen}$
X_B	$y_{Bow} = 2x^2 - x^3$ $x = \alpha LE_e(T_{ws})/LE_{pen}$, $y_r = LE_r/LE_{pen}$ $x_{min} = \alpha LE_e(T_{ws})/LE_{max}$ $X = (x - x_{min})/(1 - x_{min})$ $X_B = 2X^2 - X^3$	LE_{XB}	$X_B \cdot LE_{pen}$
y_{HT}	$x = LE_e(T_a)/LE_{pen}$, $y_r = LE_r/LE_{pen}$ y_{HT} given by (12) - (15)	LE_{HT}	$y_{HT} \cdot LE_{pen}$

are those with > 99.9% land within the grid cell). ERA5 data can be downloaded from ECMWF (<https://cds.climate.copernicus.eu>).

Monthly-average data from 2017 and 2018 for the odd-numbered months (January, March, etc.) were downloaded from ECMWF ([https://cds.climate.copernicus.eu/#!/search?text = ERA5&type = dataset](https://cds.climate.copernicus.eu/#!/search?text=ERA5&type=dataset)) as were hourly data from January 1, April 1, July 1, and October 1 in 1999, which were used to find daily average values for these four days. Downloaded data include latent and sensible heat fluxes, 2 m air temperature, 10 m wind speed, 2 m dewpoint temperature, z_0 , and a land/sea mask layer for each cell across the globe. Available energy was taken to be the same as the sum of latent and sensible heat fluxes.

3. Calculations

Section 3.1 will describe calculations and assumptions for the eddy-covariance data and section 3.2 will describe them for the ERA5 data.

3.1. Calculations for flux station data

Separate data files are provided by FLUXNET for daily, weekly, monthly, and yearly averaging times. In each, averaging periods were removed for which $H < 0$, $LE < 0$, or $R_n - G < 0$, $T_a < 0$ °C, or for times when no data were available for any of the mentioned variables or for pressure or vapor pressure deficit. Data with time-averaged wind speeds $< 1 \text{ m s}^{-1}$ were omitted because there may be poor connection between the state of the land surface and the lower atmosphere when turbulence is weak or absent, violating a basic assumption of the CR (e. g., Crago and Qualls, 2018); under such conditions LE is likely small, so impact of the removal of these data points is minimal. It was assumed that $d_0/z_0 = 4.8$ and $z_{0v} = z_0/15$ (c.f. Brutsaert, 1982, 2005; Zhang et al., 2017). The momentum roughness length was taken as the log-average value of z_0 found by Crago and Qualls (2018) for each site from the measured values of u_* . Optimal parameter values [α and, for (12), b_{HT}] were those values that minimized root mean square error (RMSE) between estimates and reference values. Reference values for dimensionless evaporation rates were found using $y = LE_r/LE_{pen}$.

Parameters were fit using a trial and error procedure. Note that the Han and Tian formulation [(12)-(15)] required fitting of two parameters. Since both parameters have significant effects on the RMSE, satisfactory results came from searching the entire range of parameter values to find optimal parameters.

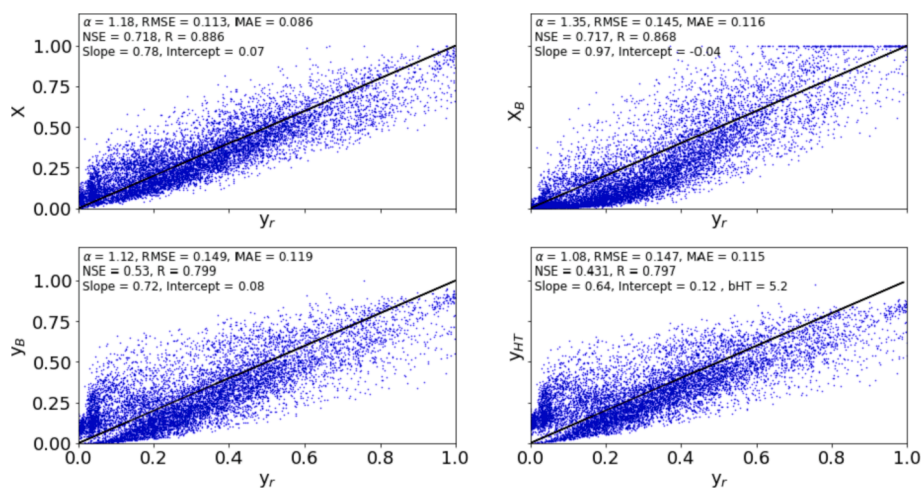


Fig. 1. Daily dimensionless evaporation rates from seven flux stations in Australia. The black lines are one-to-one. RMSE is root mean square error; MAE is mean absolute error; NSE is the Nash Sutcliffe Efficiency, R is correlation coefficient, bHT is b_{HT} , and Slope and Intercept are coefficients of the linear regression equation $y = Slope * x + Intercept$ where x represents reference estimates and y represents model values.

3.2. Calculations for ERA5 data

Technical documentation on the ECMWF website (<https://www.ecmwf.int/en/publications/ifs-documentation>, “IFS Documentation, CY41R2, Part IV, Physical Processes) explains that surface air temperatures (wind speeds) are located at a height of $z = 2 \text{ m}$ (10 m), z_0 should be 0.03 m or the given z_0 for the cell, whichever is less, and z_{0v} should be 1/10 of the resulting z_0 . Displacement height is ignored in this procedure.

For calibration of parameter values, a procedure similar to the one described above for the flux station data was used. However, with 1.4 million land cells available during the 12 months, calibration was streamlined by using a random sample (drawn without replacement) of 100,000 cells drawn from all twelve months of data. A sample of 100,000 daily cell values was also drawn from the four days in 2019.

4. Results and discussion

4.1. Results

The results are presented graphically in Figs. 1-14. Statistics relating estimates to reference values are provided inside the graphs. Statistics include RMSE (root mean square error), MAE (mean absolute error), NSE [Nash-Sutcliffe efficiency (Nash and Sutcliffe, 1970)], R (correlation coefficient), and the slope and intercept of the linear regression between model and reference values.

Figs. 1 through 14 all suggest that all four CR versions adequately estimate latent heat fluxes at these sites at daily, weekly, monthly, and yearly time scales; this is the case with flux station as well ERA5 reanalysis data. Section 4.2 will discuss Questions 1 through 5 in turn.

4.2. Discussion

4.2.1. Discussion of Question 1

Question 1 asks whether greater spatial and temporal averaging will result in smaller model errors. This can be addressed by looking at panels a and b of both Figs. 13 and 14. In both figures, the left column (panels a, c and e) considers dimensionless evaporation (LE/LE_p) and the right column (panels b, d and f) considers actual (dimensional) evaporation (LE). The top rows consider RMSE, the second rows consider α , and the third rows consider correlation coefficient R.

Panels a and b of Figs. 13 and 14 show that all the versions have a clear trend towards lower RMSE with longer averaging times. Moving from daily to weekly (Fig. 13 panel a), y_B , y_{HT} , and E_{HT} have a slight

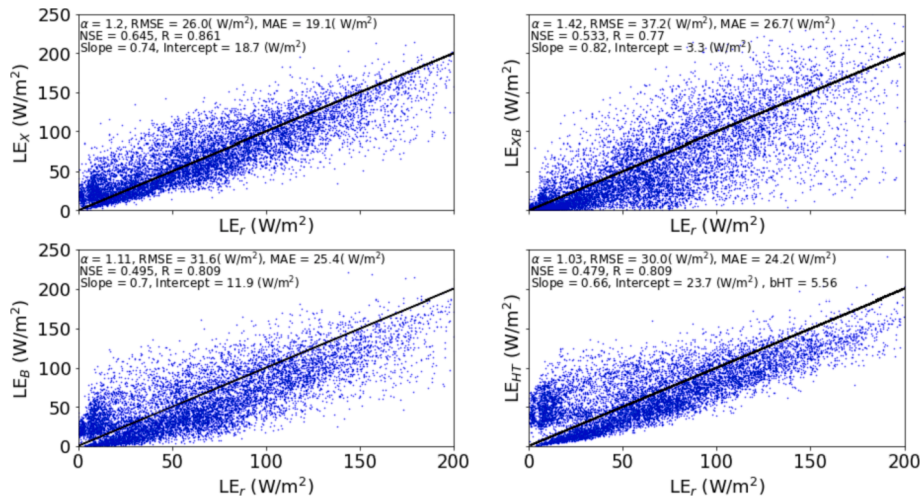


Fig. 2. Same as Fig. 1 but for dimensional evaporation.

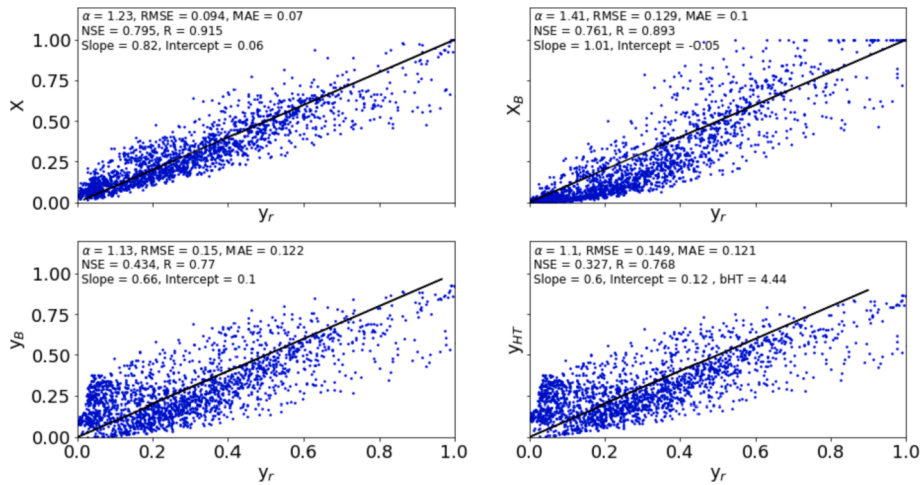


Fig. 3. Same as Fig. 1 but for weekly data.

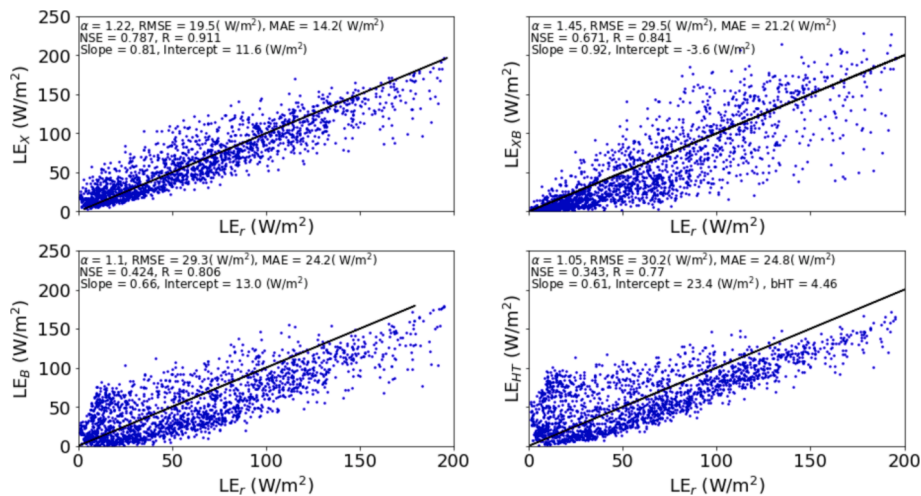


Fig. 4. Same as Fig. 2 but for weekly data.

increase in RMSE with the flux station data, but each of these versions still has a clear trend of decreasing RMSE overall. McMahon et al. (2013) note that evaporation methods using potential evaporation tend to work

best with averaging times around a month. Their observation is consistent with this result, although there is continued improvement from monthly to yearly RMSE values (Fig. 13).

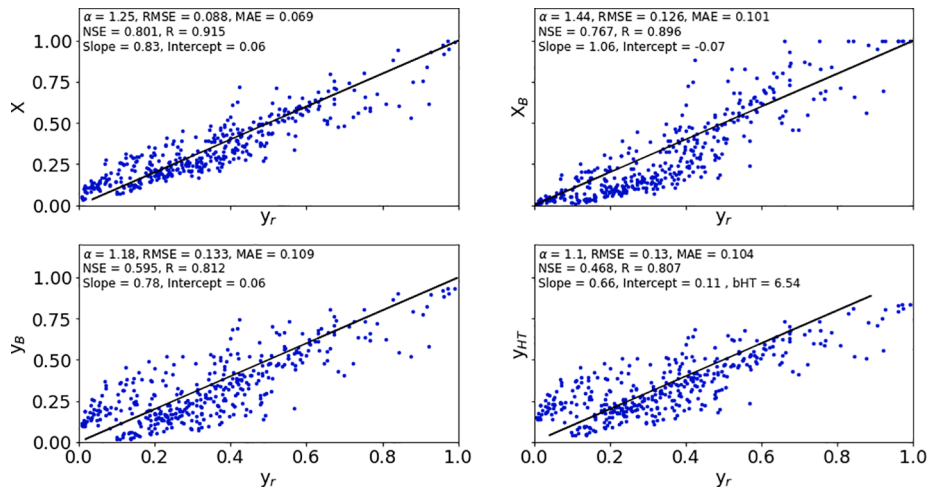


Fig. 5. Same as Fig. 1 but for monthly data.

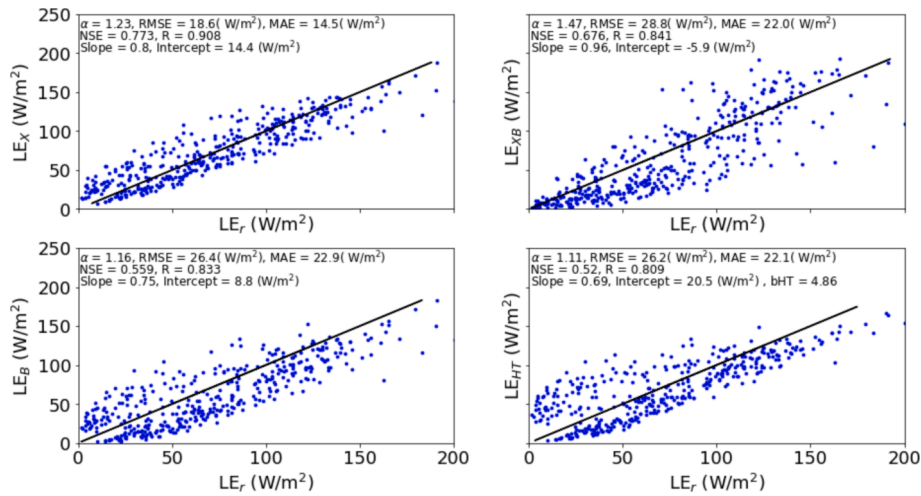


Fig. 6. Same as Fig. 2 but for monthly data.

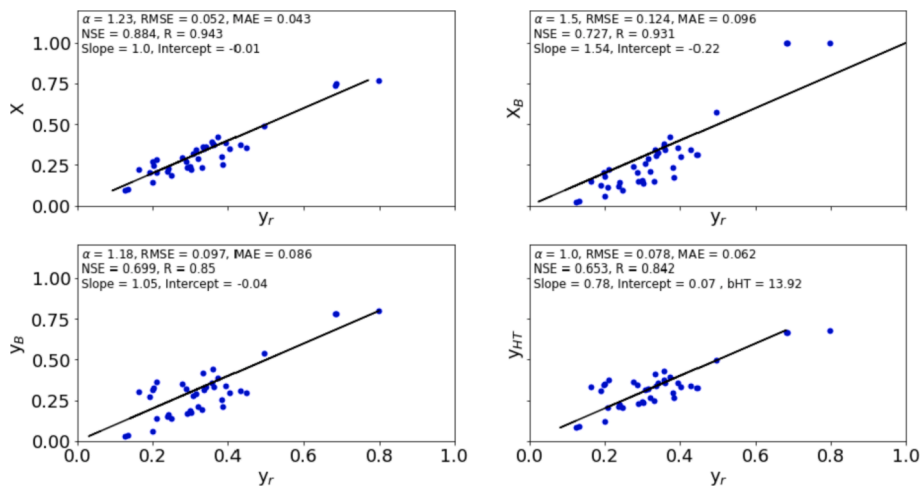


Fig. 7. Same as Fig. 1 but for yearly data.

Evaluation of changes in RMSE with increasing spatial scale requires comparison of ERA5 and flux station results. This direct comparison is not straightforward. While reanalysis data might often be considered more accurate than either model results or measurements alone (e.g.,

Szilagy et al., 2014), the ERA-Interim (the predecessor data product to ERA5; see Dee et al., 2011) land surface evaporation rates compared more poorly with the long-term water balance estimate of evaporation (precipitation minus streamflow) for HUC-6 and HUC-8 watersheds in

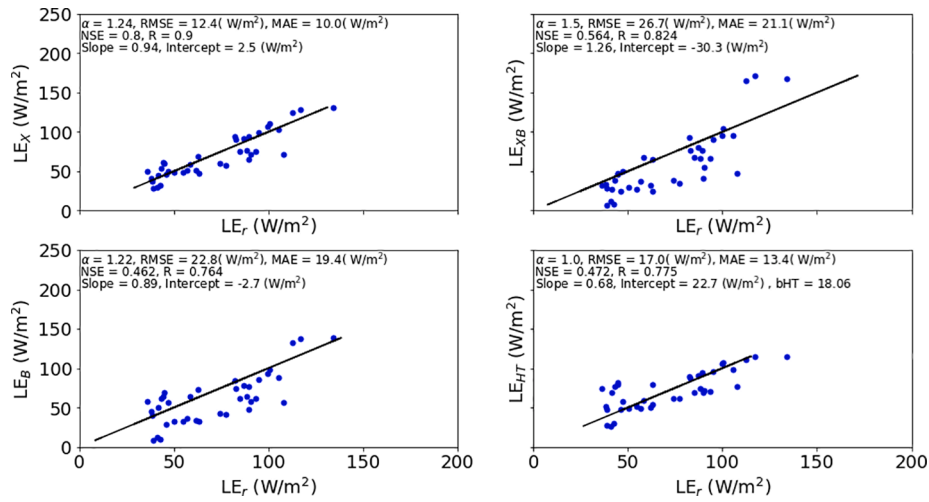


Fig. 8. Same as Fig. 2 but for yearly data.

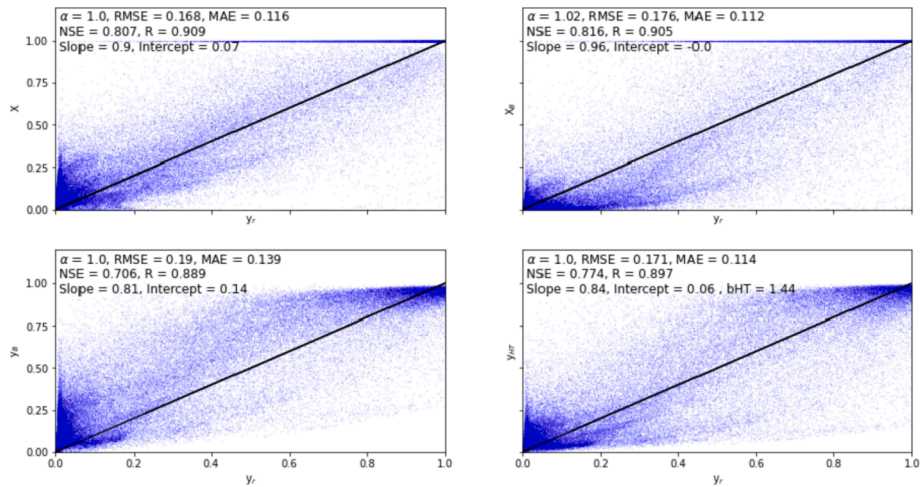


Fig. 9. Same as Fig. 1 except using the ERA5 daily data. Points plotted are a random sample of 100,000 points drawn from the 4 days of data.

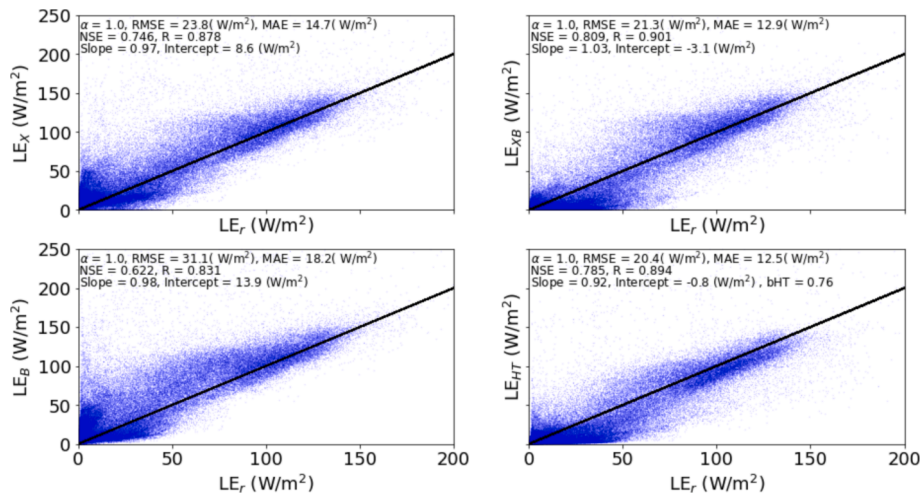


Fig. 10. Same as Fig. 9 except for dimensional evaporation.

the contiguous United States than one of the CR methods (Ma and Szilagyi, 2019). Specifically, they compared a version related to the present E_{XB} formulation to multiple other models and data products, including

the ERA-Interim gridded evaporation product. They found that ERA-Interim tended to systematically overestimate the water-balance-based evaporation estimates, while the CR-based approach had the lowest

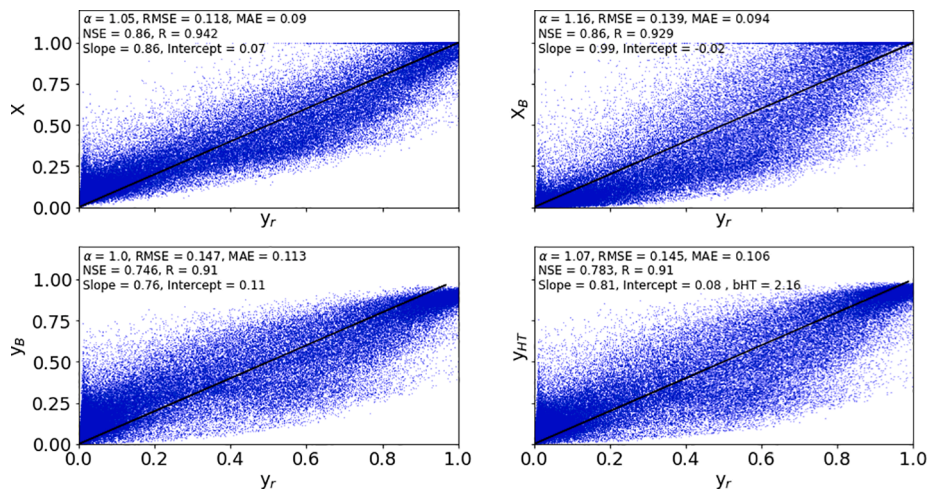


Fig. 11. Same as Fig. 9 except for monthly data.

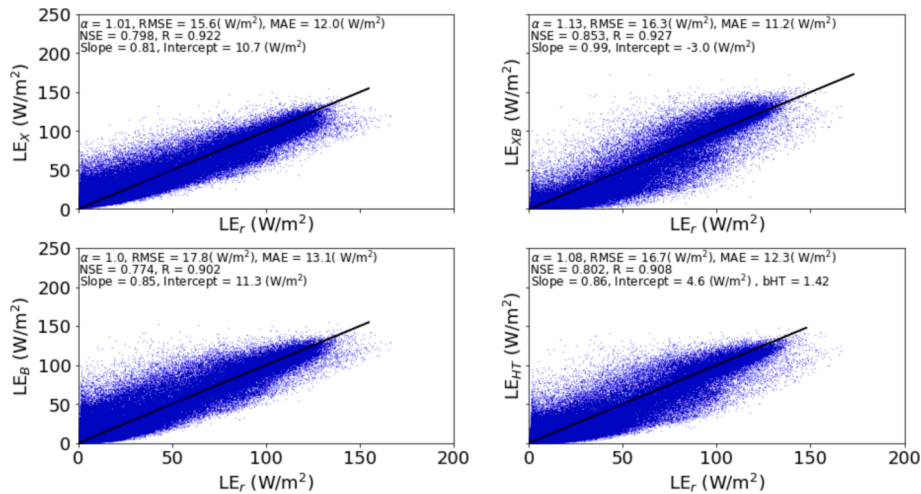


Fig. 12. Same as Fig. 11 except for dimensional evaporation.

RMSE and smallest relative bias of all the models or products they tested. Ma et al. (2019) noted similar problems with ERA-Interim evaporation estimates in China.

In Ma and Szilagyi (2019) and Ma et al. (2019), the input variables (temperature, wind speed, net radiation, etc.) came from different sources than the evaporation rates. In this study, ERA5-derived data are used to try to predict ERA5 evaporation rates. The reanalysis process in ERA5 ensures that there will at least be internal consistency between the driving variables and the fluxes, which was not necessarily the case with the Ma and Szilagyi (2019) and Ma et al. (2019) studies, because they derived driving variables from multiple sources other than ERA-Interim. It should be possible to glean at least some information about the effects of spatial scaling on the CR by comparing performance of CR versions from surface station data with that from ERA5 data, where both datasets used the same averaging time.

With this caveat regarding direct comparison, examination of Fig. 14, panels a and b, shows that dimensionless evaporation (Fig. 14 panel a) and dimensional evaporation (Fig. 14 panel b) have opposite trends with increasing averaging times. That is, dimensionless evaporation RMSE increases and dimensional evaporation RMSE decreases when moving from flux station to ERA5 data. This is true at both daily and monthly time steps and for all four versions. However, LE_B had only very small decreases between daily flux station and daily ERA5 RMSE values.

In summary, with respect to increasing temporal averaging time, RMSE does seem to decrease with greater averaging with all the of the CR versions. With respect to increasing spatial averaging, errors increase for ERA5 compared to flux station data for dimensionless evaporation, but they decrease for dimensional evaporation.

4.2.2. Discussion of Question 2

Question 2 asked if the range of the input variables would be compressed with increased averaging time, resulting in a compressed range of output values as well. Comparison of the range of data points in the corresponding plots in Figs. 1-12 supports this hypothesis. This is particularly striking when comparing Figs. 1 and 7 (dimensionless) and 2 and 8 (dimensional), which are at daily and yearly time scales, respectively. Both dimensional and dimensionless evaporation rates, for all the CR versions, show wider ranges in Fig. 1 than in 7. The compression is more obvious in the dimensional evaporation than in the dimensionless. It is also apparent in comparing daily (Figs. 9 and 10) with monthly (Figs. 11 and 12) ERA5 data.

This might explain why R values trend generally upward with increasing averaging time (dimensionless evaporation in Fig. 13, panel e) or have no clear pattern (dimensional evaporation in Fig. 13 panel f), while RMSE values in Fig. 13 generally trend downward with increasing time scales for both dimensional (panel a) and dimensionless (panel b) evaporation. While the scatter of the values might be reduced (lower

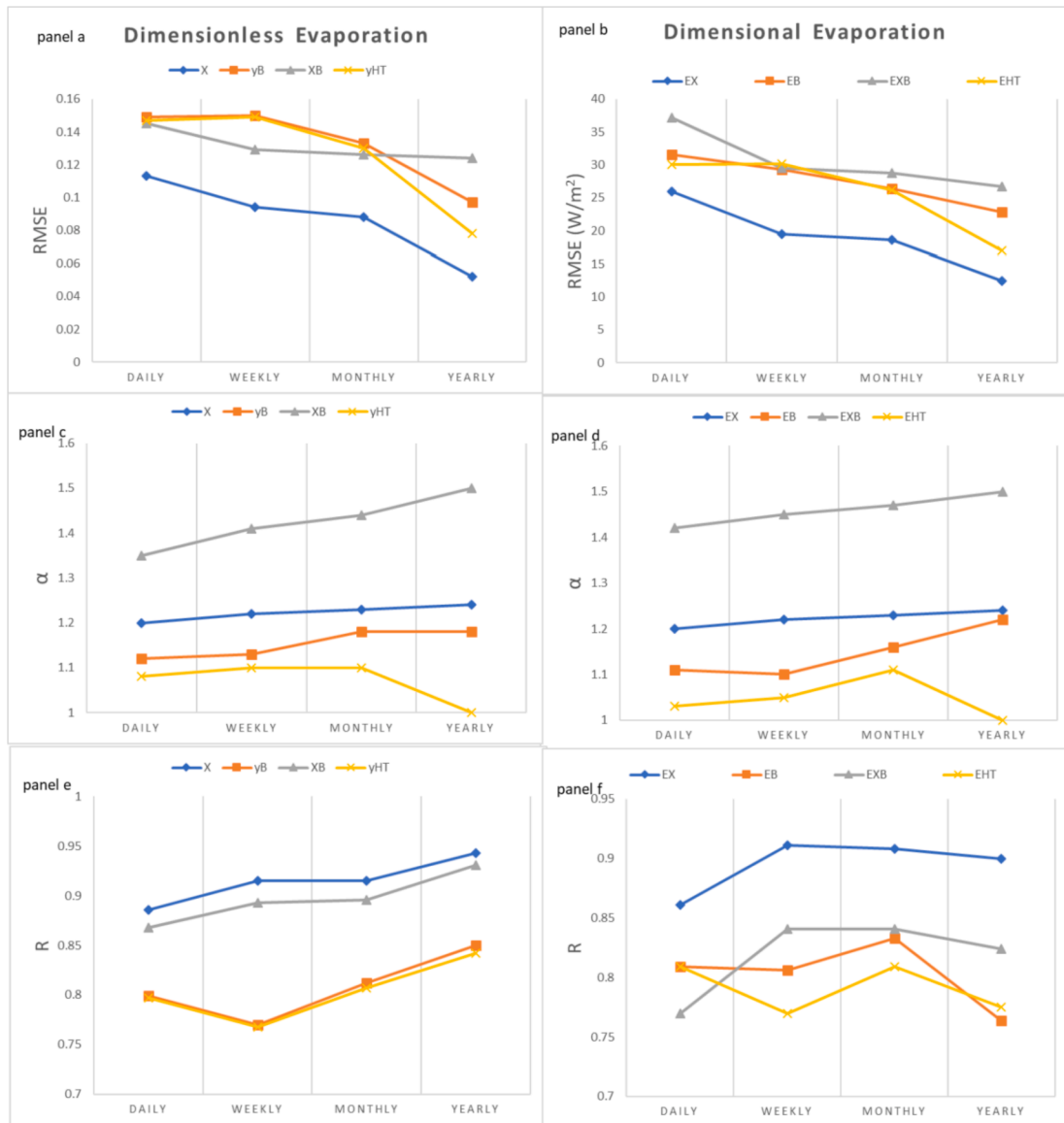


Fig. 13. Comparison of model versions with time scale for eddy-covariance flux data. Left column of panels is dimensionless evaporation and the right column is dimensional.

RMSE in panels a and b) that doesn't necessarily result in a stronger linear relationship if the range of values is reduced (Fig. 13 panels e and f).

Note that the present datasets do not provide a good way to test whether similar compression of values occurs when spatial averaging increases. This is because the flux station data come from seven specific sites, which limits the range of fluxes expected, while the ERA5 data span the globe and thus have considerably greater range in both input and output variables.

4.2.3. Discussion of Question 3

Question 3 asks whether the effects of advection will be smaller at larger spatial scales. Fig. 14, panels c and d can be used to address this question. This figure shows that at both the daily and monthly averaging times, α does in fact decrease when moving from the flux station data to the larger-spatial-scale ERA5 data. While this is the finding predicted by the hypothesis, the substantial differences between the nature of the flux station datasets and the ERA5 dataset (discussed earlier) makes it difficult to conclude that the hypothesis is supported.

Furthermore, the role of α in the context of the CR is not obvious.

Note that the calibrated value of α is at the physically-realistic lower bound of 1 (see Priestley & Taylor, 1972) for many of the versions. This value of α corresponds to zero advection effect. Even with much larger spatial averaging areas, it is expected that some advection will be present due to entrainment of free atmospheric air into the ABL [e.g., McNaughton and Spriggs (1989), Lhomme and Guilioni (2006), Lhomme and Guilioni (2010), Raupach (2001)]. This suggests that the reanalysis data might be consistent with the specific land surface evaporation model used in the reanalysis, but that model may not fully describe the physical process of evaporation, particularly over inhomogeneous surfaces. At the opposite extreme, values of α exceeding 1.4 (near the upper limit of the typical range for α) are found for X_B and LLE_{XB} versions with both flux station and ERA5 data. Note that these values of α are much lower for X_B and LLE_{XB} when the original Penman (1948) wind function is used in place of (5).

Brutsaert et al. (2016) stated that α as used in CR formulations "is not quite the Priestley-Taylor parameter, but merely a weak analog of it." Thus, α could be viewed simply as a tunable parameter, such that values of $\alpha < 1$ are viewed as acceptable. However, the present authors take the view that α in the CR should be treated as a close analog to the Priestley-

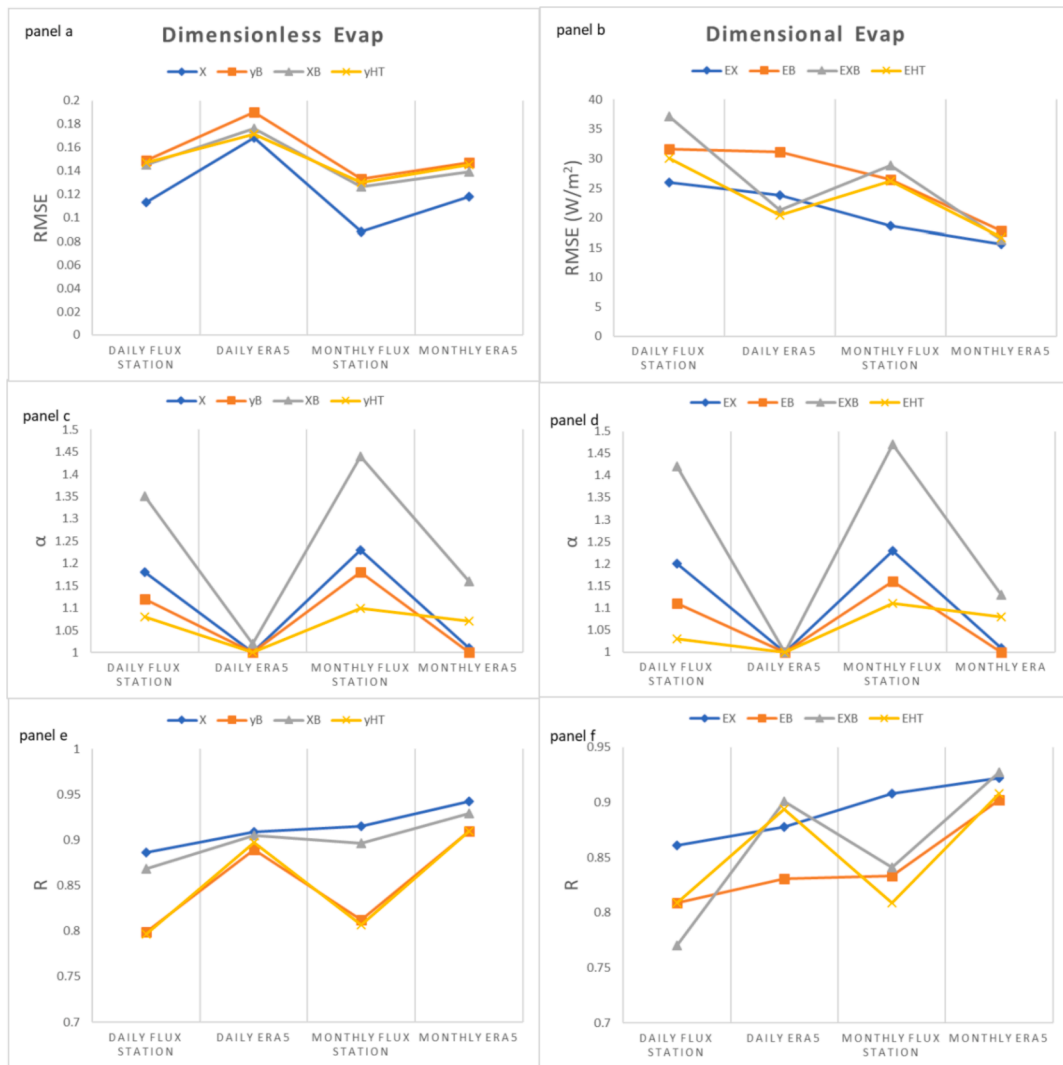


Fig. 14. Comparison of eddy-covariance flux results and ERA5 results at daily and monthly time-scales. The left column of panels is dimensionless evaporation and the right column is dimensional.

Taylor parameter. For this reason, $\alpha = 1$ was taken as the minimum allowed value in this study. Thus, the direction of the trends in α with increasing spatial scale are those expected if advection is in fact less pronounced at larger spatial scales. However, the very low values of α with ERA5, and large values of α with the X_B (LE_{XB}) version make these results rather uncertain.

4.2.4. Question 4

Question 4 asks whether the same CR versions that work well at predicting dimensionless evaporation rates will also work well predicting dimensional rates. All the CR versions considered here are formulated in terms of the dimensionless variables $x = \alpha LE_e / LE_p$ and $y = LE / LE_p$ (except for y_{HT} and LLE_{HT} which are formulated in terms of x/α and y). For example, Brutsaert's (2015) version follows a prescribed third-order polynomial across the (x, y) space, and the other versions all use another algorithm to translate from a value of x to a value of y . Thus, it is legitimate to verify these CR versions in terms of how well predicted values of y match reference values of y . Dimensional evaporation is found by multiplying the predicted y by LE_p , so this question asks whether the same versions that best predict y also accurately predict LE .

In order to incorporate several different statistics into a holistic index of CR version performance, RMSE, R and Slope (specifically, the absolute difference between the regression slope and 1) were chosen as key

performance variables. For each dataset (i.e., Flux Station or ERA5) and each averaging time, versions were ranked from best (rank 1) to worst (rank 4) for each of these performance variables and then the ranks of these three variables were summed for all the time scales. First, flux station data were considered separately from ERA5 data, and then the two sets were combined. The results are shown in Table 2.

To address question four, model versions based on the same underlying equation relating x and y , for example, X and LE_X , will be denoted (X, LLE_X) . Based on Table 2, for both flux station and ERA5 data, the (X, LE_X) and the (X_B, LE_{XB}) versions are always ranked 1 or 2, and the (y_B, LE_B) and (y_{HT}, LLE_{HT}) versions are always ranked 3 or 4 for both dimensional and dimensionless evaporation. This is true for each of the last three columns of Table 2. In fact, the overall rankings for dimensionless and dimensional evaporation (last column of Table 2) both follow the same pattern (from ranks 1 to 4): (X, LE_X) , (X_B, LE_{XB}) , (y_B, LE_B) , (y_{HT}, LE_{HT}) ; the exception is that LE_B and LE_{HT} tie with a rank of 3. Thus, with the versions tested in Table 2, a version's skill at predicting dimensionless evaporation corresponds well to skill also in predicting dimensional evaporation.

Versions were also tested (detailed results not included) in which LE_p was calculated in two different ways. One method is based on Qualls and Crago (2020); see also Crago and Qualls, (2021) for an application to CR versions], who noted that a variable similar to T_{ws} can be derived from

Table 2
Sum of Flux station ranks and ERA5 ranks, and overall ranks of CR versions.

	Eddy-Covariance Rank Total	ERA5 Rank Total	Combined Rank Total	Eddy-Covariance Rank	ERA5 Rank	Overall Rank
X	15	8	23	1	1	1
y _B	38	23	61	3	3	3
X _B	25	11	36	2	2	2
y _{HT}	42	17	59	4	3	4
LE _X	15	16	31	1	2	1
LE _B	34	20	54	3	4	3
LE _{X_B}	31	9	40	2	1	2
LE _{HT}	39	15	54	4	3	3

(1), in which H and LE are written as energy and mass transfer equations driven by the difference in potential temperature and vapor pressure (respectively) between the ground and the measurement height. When available energy, wind speed, air temperature, air humidity, z_0 , d_0 , and z_{0v} are all known, the equation can be solved numerically for the unknown surface temperature (T_{0w}). An apparent wet surface evaporation rate LE_{0w} can then be found by using T_{0w} as the ground temperature in the mass transfer equation. LE_{max} can be found from the mass transfer equation with $e_a = 0$. When this method is used to develop X in the $y = X$ version, RMSE is the smallest of all the models; however, LE_X is then ranked in the bottom half of the methods.

Another method to calculate LE_p is to use the Penman equation (2) with the original wind function proposed by Penman (1948), of the form $f(u) = a + b \cdot u$ where a and b are constants. The LE_{max} is then estimated using (2) with the Penman wind function and using T_{dry} as discussed below equation (9). When these LE_p and LE_{max} values are used in the y_{HT} version, the results were relatively poor, but the same version produced LE_{HT} values that ranked near the top. Actually, the dimensionless evaporation for the CR versions considered was nearly always improved by estimating LE_p with LE_{0w} , but at the cost of lower performance with dimensional evaporation. Similarly, CR performance could be improved for dimensional evaporation by using the LE_p with the original Penman wind function, but at the expense of relatively poor dimensionless estimates.

It is clearly desirable that versions that have skill in predicting dimensionless evaporation also have skill in predicting dimensional evaporation. While the current versions, in which LE_p is given by Penman's equation with the MOS wind function, has this desirable property, it cannot be taken for granted. The four basic versions examined here do not seem in themselves to be biased in favor of either dimensional or dimensionless evaporation, but some methods of estimating LE_p (and LE_{max}) do seem to favor one or the other. Detailed results are not presented here in order to maintain a focus on the four basic CR versions, rather than on different LE_p equations.

4.2.5. Question 5

Question 5 asks whether some versions of the CR are consistently better at predicting evaporation. Reference to Table 1 suggests that the two versions based on the rescaling of the CR suggested by Crago et al. (2016) [(X, LE_X) and (X_B, LE_{X_B})] do perform better overall than the other two versions.

Note that in a previous draft of this paper, LE_p was taken either to be equal to LE_{0w} (described in section 4.2.4) or it was given by (2) with the original Penman (1948) wind function. In this case, the (X_B, LE_{X_B}) version with the LE_p given by (2) with the Penman (1948) wind function and the (y_{HT}, LE_{HT}) model with the same LE_p both performed well for dimensional evaporation. In fact, that particular configuration of (X_B, LE_{X_B}) ranked highest overall. While this study focuses on four basic CR versions, clearly the formulation of the LE_p used is also important.

5. Conclusions

Measurements from eddy-covariance flux stations averaged over daily, weekly, monthly, and yearly time scales, and global data

downloaded from the ERA5 reanalysis at daily and monthly averaging times were used to evaluate several CR versions. The purpose was to determine whether the temporal and spatial averaging has a significant impact on the results and on the relative performance of the various models. The study was conducted to evaluate the five questions asked in the introduction.

Question 1 asked whether averaging over larger time and space scales should reduce RMSE values. In the case of time averaging, this was in fact the case for each of the CR versions for both flux station and ERA5 data. For spatial averaging, the study results were inconclusive.

Question 2 asked whether larger averaging times would also reduce the range of the input variables and of the CR-model evaporation rates. The results suggest this is the case.

Question 3 asked whether at larger spatial scales advection would be weaker, so that the Priestley-Taylor parameter α would be smaller at larger spatial scales. While CR model results using flux station data (i.e., smaller scales) and ERA5 data (i.e., larger scale) cannot easily be compared directly, the α values at daily and monthly averaging times were both smaller for the ERA5 data than for the surface station data. While this is the finding predicted by the hypothesis, further study is needed to fully address this question.

Question 4 asked whether CR versions that best predict dimensionless evaporation are the same as those that best predict dimensional evaporation. The basic CR models $y = X$, $y = 2x^2 - x^3$, $y = 2X^2 - X^3$ and y_{HT} themselves do not seem to inherently favor either dimensional or dimensionless evaporation. However, variations on how LE_p is calculated can bias versions toward skill in either dimensionless or dimensional evaporation prediction.

Question 5 asked whether any CR versions regularly outperformed the other versions. Study results support that the rescaled versions [(X, LE_X) , (X_B, LE_{X_B})] outperformed the other versions for both dimensional and dimensionless evaporation.

Declaration of Competing Interest

The authors declare that they have no known competing financial interests or personal relationships that could have appeared to influence the work reported in this paper.

Acknowledgements

This research was supported by the BME Water Sciences & Disaster Prevention TKP2020 IE grant of NKFIH Hungary (BME IE-VIZ TKP2020).

This research has been supported in part by NIFA (USGS) grant IDA01584.

Data availability

FLUXNET data can be downloaded from fluxnet.org. ERA5 data can be downloaded from <https://www.ecmwf.int/en/forecasts/datasets/reanalysis-datasets/era5>.

References

- Andreas, Edgar, Jordan, Rachel, Mahrt, Larry, Vickers, Dean, 2013. Estimating the Bowen ratio over the open and ice-covered ocean. *J. Geophysical Research* 118, 4334–4345. <https://doi.org/10.1002/jgrc.20295>, 2013.
- Baldocchi, D., Falge, E., Gu, L., Olson, R., Hollinger, D., Running, S., Anthoni, P., Bernhofer, C.H., Davis, K., Evans, R., Fuentes, J., Goldstein, A., Katul, G., Law, B., Lee, X., Malhi, Y., Meyers, T., Munger, W., Oechel, W., Paw, K.T., Pilegaard, K., Schmid, H.P., Valentini, R., Verma, S., Vesala, T., Wilson, K., Wofsy, S., 2001. FLUXNET: A new tool to study the temporal and spatial variability of ecosystem-scale carbon dioxide, water vapor, and energy flux densities. *Bull. Am. Meteorol. Soc.* 82 (11), 2415–2434.
- Bouchet, R., 1963. Evapotranspiration réelle et potentielle, signification climatique. *Int. Assoc. Hydrol. Sci. Publicat.* 62, 134–142.
- Brutsaert, W., 1982. Evaporation into the Atmosphere: Theory, History, and Applications. D. Reidel-Kluwer.
- Brutsaert, W., 2005. *Hydrology: An Introduction*. Cambridge University Press, Cambridge, doi: 10.0-521-82479-6.
- Brutsaert, W., 2015. A generalized complementary principle with physical constraints for land-surface evaporation. *Water Resour. Res.* 51 (10), 8087–8093. <https://doi.org/10.1002/wrcr.v51.1010.1002/2015WR017720>.
- Brutsaert, W., Stricker, H., 1979. An advection-aridity approach to estimate actual regional evapotranspiration. *Water Resour. Res.* 15 (2), 443–450.
- Brutsaert, W., Li, W., Takahashi, A., Hiyama, T., Zhang, L.u., Liu, W., 2016. Nonlinear advection-aridity method for landscape evaporation and its application during the growing season in the southern Loess Plateau of the Yellow River basin. *Water Resour. Res.* 53 (1), 270–282. <https://doi.org/10.1002/2016WR019472>.
- Brutsaert, W., Cheng, L., Zhang, L., 2020. Spatial distribution of global landscape evaporation in the early twenty-first century by means of a generalized complementary approach. *J. Hydrometeorol.* 21 (2), 287–298.
- Chow, V.T., Maidment, D.R., Mays, L.W., 1988. *Applied Hydrology*. McGraw-Hill. Doi: 0070108102.
- Crago, R., Szilagyi, J., Qualls, R., Huntington, J., 2016. Rescaling the complementary relationship for land surface evaporation. *Water Resour. Res.* 52 (11), 8461–8471. <https://doi.org/10.1002/2016WR019753>.
- Crago, R., Qualls, R., Szilagyi, J., Huntington, J., 2017. Reply to comment by Ma and Zhang on “Rescaling the complementary relationship for land surface evaporation”. *Water Resour. Res.* 53 (7), 6343–6344. <https://doi.org/10.1002/2017WR021021>.
- Crago, R., Qualls, R., 2018. Evaluation of the Generalized and rescaled complementary relationships. *Water Resour. Res.* 54, 8086–8102. <https://doi.org/10.1029/2018WR023401>.
- Crago, R., Qualls, R., 2021. A graphical interpretation of the rescaled complementary relationship for evapotranspiration. *Water Resour. Res.* 57 (8) <https://doi.org/10.1029/2020WR028299>.
- Crago, R., Szilagyi, J., Qualls, R., 2020a. Comment on: “A review of the complementary principle of evaporation: from the original linear relationship to generalized nonlinear functions” by Han and Tian (2020). *Hydrol. Earth Syst. Sci.* 24, 1–6. <https://doi.org/10.5194/hess-24-1-2020>.
- Crago, R., Szilagyi, J., and Qualls, R., 2020b. Reply to “Comment on ‘Two papers about the generalized complementary relationships by Crago et al.’”, *Water Resour. Res.*, 56(3), Doi: 10.1029/2019WR026773.
- Crago, R., Szilagyi, J., Qualls, R., 2021. Comment on: “A review of the complementary principle of evaporation: from the original linear relationship to generalized nonlinear functions” by Han and Tian. *Hydrol. Earth Syst. Sci.* 25, 63–68. <https://doi.org/10.5194/hess-25-63-2021>.
- Dee, D.P., Uppala, S.M., Simmons, A.J., Berrisford, P., Poli, P., Kobayashi, S., Andrae, U., Balmaseda, M.A., Balsamo, G., Bauer, P., Bechtold, P., Beljaars, A.C.M., van de Berg, L., Bidlot, J., Bormann, N., Delsol, C., Dragani, R., Fuentes, M., Geer, A.J., Haimberger, L., Healy, S.B., Hersbach, H., Hólm, E.V., Isaksen, I., Kållberg, P., Köhler, M., Matricardi, M., McNally, A.P., Monge-Sanz, B.M., Morcrette, J.-J., Park, B.-K., Peubey, C., de Rosnay, P., Tavolato, C., Thépaut, J.-N., Vitart, F., 2011. The ERA-Interim reanalysis: Configuration and performance of the data assimilation system. *Q. J. R. Meteorol. Soc.* 137 (656), 553–597.
- Han, S., Tian, F., 2018. Derivation of a sigmoid generalized complementary function for evaporation with physical constraints. *Water Resour. Res.* 54 (7), 5050–5068. <https://doi.org/10.1029/2017WR021755>.
- Han, S., Tian, F., 2020. Complementary principle of evaporation: From original linear relationship to generalized nonlinear functions. *Hydrol. Earth Syst. Sci.* <https://doi.org/10.5194/hess-2019-545>.
- Hersbach, H., Bell, B., Berrisford, P., Hirahara, S., Horányi, A., Muñoz-Sabater, J., Nicolas, J., Peubey, C., Radu, R., Schepers, D., Simmons, A., 2020. The ERA5 global reanalysis. *Q. J. R. Meteorol. Soc.* 146 (730), 1999–2049.
- Liu, W., Zhou, H., Han, X., Li, Z., 2020. Comment on two papers about the generalized complementary evaporation relationships by Crago et al. *Water Resour. Res.* 56 (3) <https://doi.org/10.1029/2019WR026773>.
- Lhomme, J.P., Guillon, L., 2006. Comments on some articles about the complementary relationship. *J. Hydrol.* 323 (1–4), 1–3. <https://doi.org/10.1016/j.jhydrol.2005.08.014>.
- Lhomme, J.P., Guillon, L., 2010. On the link between potential evaporation and regional evaporation from a CBL perspective. *Theor. Appl. Climatol.* 101 (1–2), 143–147.
- Ma, N., Szilagyi, J., 2019. The CR of Evaporation: A Calibration-Free Diagnostic and Benchmarking Tool for Large-Scale Terrestrial Evapotranspiration Modeling. *Water Resour. Res.*, 55. Doi: 10.1029/2019WR024867.
- Ma, N., Szilagyi, J., Zhang, Y., Liu, W., 2019. Complementary-relationship-based modeling of terrestrial evapotranspiration across China during 1982–2012: Validation and spatiotemporal analyses. *J. Geophys. Res.: Atmosph.* 124, 4326–4351. <https://doi.org/10.1029/2018JD029850>.
- Ma, N., Zhang, Y., 2017. Comment on “Rescaling the complementary relationship for land surface evaporation” by R. Crago et al. *Water Resour. Res.* 53 (7), 6340–6342. <https://doi.org/10.1002/2017WR020892>.
- Ma, N., Szilagyi, J., & Zhang, Y., 2021. Calibration-free complementary relationship estimates terrestrial evapotranspiration globally. *Water Resour. Res.*, 57(9), e2021WR029691.
- McMahon, T.A., Peel, M.C., Lowe, L., Srikanthan, R., McVicar, T.R., 2013. Estimating actual, potential, reference crop and pan evaporation using standard meteorological data: A pragmatic synthesis. *Hydrol. Earth Syst. Sci.* 17 (4), 1331–1363.
- McNaughton, K.G. and Spriggs, T.W., 1989. An evaluation of the Priestley and Taylor equation and the complementary relationship using results from a mixed-layer model of the convective boundary layer, Estimation of Areal Evapotranspiration, IAHS Publ no. 177, 89–104. Doi: 10.1016/0022-1694(70)90255-6.
- Nash, J.E., Sutcliffe, J.V., 1970. River Flow Forecasting through Conceptual Model. Part 1—A Discussion of Principles. *J. Hydrol.* 10, 282–290.
- Pastorello, G., Trotta, C. others, 2020. The FLUXNET2015 dataset and the ONEFlux processing pipeline for eddy covariance data, *Scient. Data* (7: 225), doi:10.1038/s41597-020-0534-3.
- Penman, H. L., 1948. Natural evaporation from open water, bare soil and grass, *Proceed. Roy. Soc. London, Series A, Mathemat. Phys. Sci.*, 193, 120–145.
- Priestley, C.H.B., Taylor, R.J., 1972. On the assessment of surface heat flux and evaporation using large-scale parameters. *Mon. Weather Rev.* 100 (2), 81–92.
- Qualls, R.J., Crago, R.D., 2020. Graphical interpretation of wet surface evaporation equations. *Water Resour. Res.* 56 (10) <https://doi.org/10.1029/2019WR026766>.
- Raupach, M.R., 2001. Combination theory and equilibrium evaporation. *Q. J. R. Meteorol. Soc.* 127 (574), 1149–1181.
- Slatyer, R.O. and McIlroy, I.C., 1961. Practical microclimatology, with special reference to the water factor in soil-plant atmosphere relationships. *Practical microclimatology, with special reference to the water factor in soil-plant atmosphere relationships*, Melbourne, C.S.I.R.O., pp. 307.
- Stull, R. B., 1988. *An Introduction to Boundary Layer Meteorology*. Kluwer, Boston, doi: 10:902727694.
- Szilagyi, J., Jozsa, J., 2008. New findings about the complementary relationship-based evaporation estimation methods. *J. Hydrol.* 354 (1–4), 171–186.
- Szilagyi, J., Schepers, A., 2014. Coupled heat and vapor transport: The thermostat effect of a freely evaporating land surface. *Geophys. Res. Lett.* 41 (2), 435–441. <https://doi.org/10.1002/2013GL058979>.
- Szilagyi, J., Parlange, M.B., Katul, G.G., 2014. Assessment of the Priestley-Taylor parameter value from ERA-Interim Global reanalysis data. *J. Hydrol. Environ. Res.* 2, 1–7.
- Szilagyi, J., 2015. Complementary-relationship-based 30 year normal (1981–2010) of monthly latent heat fluxes across the contiguous United States. *Water Resour. Res.* 51, 9367–9377.
- Szilagyi, J., Crago, R., Qualls, R.J., 2016. Testing the generalized complementary relationship of evaporation with continental-scale long-term water-balance data. *J. Hydrol.* 540, 914–922.
- Szilagyi, J., Crago, R., Qualls, R., 2017. A calibration-free formulation of the complementary relationship of evaporation for continental-scale hydrology. *J. Geophys. Res.: Atmospheres* 122, 264–278.
- Szilagyi, J., Crago, R., 2019. Comment on “Derivation of a sigmoid generalized complementary function for evaporation with physical constraints” by Han and Tian. *Water Resour. Res.* 55, 868–869.
- Zhang, L.u., Cheng, L., Brutsaert, W., 2017. Estimation of land surface evaporation using a generalized nonlinear complementary relationship. *J. Geophys. Research: Atmospheres* 122 (3), 1475–1487.